Statistically reliable 'Atomistic' Simulation of Sub 100 nm MOSFETs

A. Asenov

Device Modelling Group, Department of Electronics and Electrical Engineering
The University of Glasgow, Glasgow G12 8LT, Scotland, UK

Abstract

A 3D 'atomistic' simulation technique to study random impurity induced threshold voltage lowering and fluctuations in sub 0.1 μm MOSFETs is presented. It allows statistical analysis of random impurity effects down to the individual impurity level. Efficient algorithms based on a single solution of Poisson's equation, followed by the solution of a simplified current continuity equation are used in the simulations.

1. Introduction

At the end of the Silicon Roadmap the MOSFET channel length will be below 50 nm [1]. Random fluctuations of a small numbers of impurities and their microscopic arrangement in the channel depletion layer of sub-100 nm MOSFETs will cause an average decrease and spread in the threshold voltage, degradation of the subthreshold slope and variations in the output current [2, 3]. The discrete stochastic distribution of impurity atoms results in 3D potential and current distributions and requires 3D simulations with fine grain discretization. Statistically significant samples of microscopically different devices have to be simulated in order to understand the trends in the variation of the parameters and to build up a reliable statistics on which the IC design and optimisation should be based. This is a computationally demanding task and very few 3D simulation studies of discrete impurity fluctuation effects have been published up to date [4, 5], all based on small samples. In this paper, for the first time we present a large scale statistical 3D simulation results of 'atomistic' discrete impurity fluctuation effects in sub-100 nm MOSFETs.

2. Simulation technique

The analysis is focused on the random impurity induced threshold voltage lowering and fluctuations. The simulations and the extraction of the threshold voltage are carried out in the subthreshold region at low drain voltage. They are based on a single solution of the Poisson equation and a modified current continuity equation for each bias point. Current

criterion and effective search algorithms are used to determine the threshold voltage. The potential distributions in a 50x50 nm MOSFET resulting from continuous charge density and random impurities are compared in Figs 1 *a,b*. In the solution domain of Fig. 1 b the random impurities 'atomistic' region extends from the source to the drain. The average number of impurities in this region is calculated by integrating the continuous doping distribution within it. The actual number of impurities is chosen from a Poisson distribution with a mean equal to the calculated average impurity number. Impurities with a probability distribution, corresponding to the continuous doping distribution, are placed randomly in the 'atomistic' region using a rejection technique. The impurities are assigned to the nearest point of the grid, introducing a charge density q/h^3.

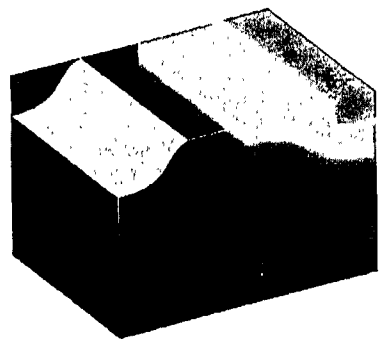

Fig. 1 (a) Potential distribution in a 50x50 nm uniformly doped MOSFET. $V_G = 0.4$ V. $N_D = 5\text{x}10^{18}$ cm^{-3} $t_{ox} = 3$ nm.

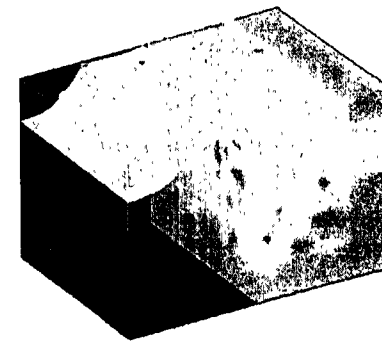

Fig. 1 (b) Potential distribution in a 50x50 nm 'atomisticaly' doped MOSFET. $V_G = 0.4$ V. $N_D = 5\text{x}10^{18}$ cm^{-3} $t_{ox} = 3$ nm.

The Poisson equation at a particular gate voltage is solved for a zero voltage applied between the source and the drain. Then, in the case of an n-channel MOSFET for example, the current density J_n associated with low applied drain voltage V_D is calculated by solving the continuity equation $\nabla . J_n = 0$ with $J_n = \sigma_n E_V$ where σ_n is the local conductivity and E_V is the electric field associated with the applied drain voltage. This leads to the following elliptical equation for the potential V driving the current:

$$\nabla . \mu_n n \nabla V = 0 \qquad (1)$$

where μ_n is the electron mobility and n is the electron concentration calculated from the solution of Poisson's equation. For properly scaled MOSFETs it is usually enough to solve Eq. (1) in a solution domain extending from the Si/SiO_2 interface down to less than 10 nm in the semiconductor. The boundary conditions are: $V = 0$ at the source, $V = V_D$ at the drain contact, and zero normal derivative at all other boundaries. In contrast to the standard drift-diffusion equation, the discretization of Eq. (1) leads to a symmetrical positive definite matrix which can be solved using standard iterative techniques.

Approximately three hours are required on a PowerMouse 4 processor Parsytec system, to accumulate statistics for the threshold voltage in a sample of 200 microscopically different MOSFETs with a 50x50x70 nodes grid.

Results and discussion

Our approach is illustrated in the simulation of MOSFETs with oxide thickness 30 nm, junction depth 7 nm channel width 50 nm and various channel lengths. The doping concentration in the channel region is $5x10^{18}$ cm^{-3}. Fig. 2 illustrates the subthreshold characteristics of 50 MOSFETs with channel width 50 nm and effective channel length 50 nm, calculated at low drain voltage. It summarises most of the effects associated with the random discrete impurities. The spread in the device characteristics is accompanied with a lowering in the average threshold voltage and a slight reduction in the subthreshold slope.

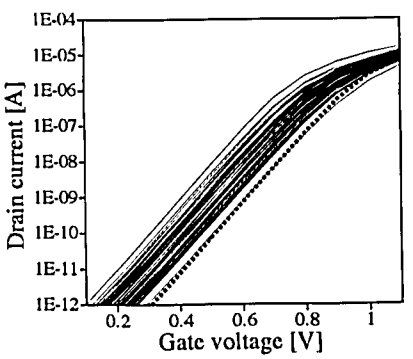

Fig. 2. I_D-V_G characteristics of 50 'atomistically' simulated 50x50 nm MOSFETs nm MOSFETs . The dashed line represents a device with continuous doping. $N_D = 5x10^{18}$ cm^{-3} and $t_{ox} = 3$ nm.

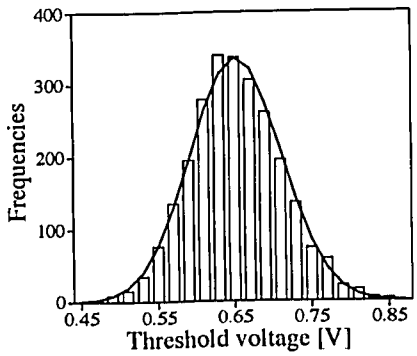

Fig. 3. Threshold voltage frequency distribution for a random sample of 2500 microscopically different 50x50 nm MOSFETs. $N_D = 5x10^{18}$ cm^{-3} and $t_{ox} = 3$ nm.

To test the hypothesis that the random impurity induced threshold voltage fluctuations follow a normal distribution we use a sample of 2500 microscopically different 50x50 nm MOSFETs with $N_D = 5x10^{18}$ cm^{-3} and $t_{ox} = 3$ nm. The threshold voltage frequency distribution and the corresponding normal distribution are compared in Fig. 3. The goodness of fit for the data is excellent with χ^2 probability $p(X > \chi^2) = 0.21$. There is, however, a visual indication that the threshold voltage distribution is slightly positively skewed. This is confirmed by the calculated Pearson second coefficient of skewness which has a value of 0.13 for the above data.

The 'atomistically' simulated average threshold voltage $\langle V_T \rangle$ for a set of MOSFETs with different channel lengths is compared in Fig. 4 to the threshold voltage V_{T0} of devices with continuous doping. In the same picture, as an insert, the difference between V_{T0} and $\langle V_T \rangle$ is also shown. The 'atomistic' simulations predict lowering in the threshold voltage compared to continuous doping simulations. The lowering increases rapidly below a 50 nm effective channel length. This threshold voltage lowering will partially compensate the increase in the threshold voltage associated with quantum mechanical effects in short, heavily doped MOSFETs, which are not taken into account in our simulations.

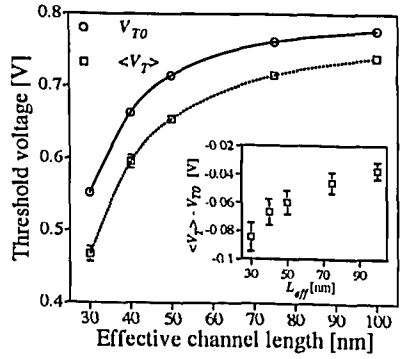

Fig. 4. Comparison of 'atomistically' simulated average threshold voltage $\langle V_T \rangle$ and the threshold voltage V_{T0} of MOSFETs with continuous doping for a set of MOSFETs with different channel lengths. $t_{OX} = 3$ nm $N_D = 5\text{x}10^{18}$ cm^{-3}, $W = 50$ nm. Samples of 200 transistors.

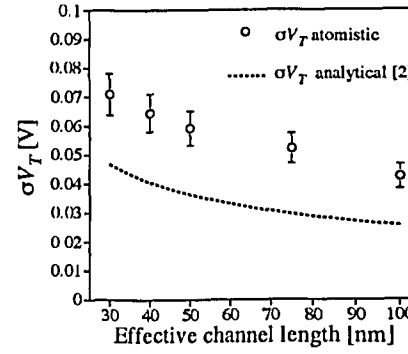

Fig. 5. Standard deviation in the threshold voltage σV_T for a set of MOSFETs with channel width 50 nm and different channel lengths. $N_D = 5\text{x}10^{18}$ cm^{-3}, $t_{OX} = 3$ nm. Samples of 200 transistors.

The standard deviation in the threshold voltage σV_T obtained from our 'atomistic' simulations is compared in Fig. 5 to the simple analytical models proposed in [2]. The atomisticaly calculated standard deviation follows the $1/\sqrt{L_{eff}}$ dependence predicted by the analytical model, but its magnitude is larger. This disagreement is possibly due to the fact that the analytical models take into account only the fluctuations in the total charge controlled by the gate, resulting from the dopant number fluctuations in the depletion layer, but do not incorporate effects associated with the random microscopic arrangements of the individual dopants.

References

[1] "The National Technology Road-map for Semiconductors", *Semiconductor Industry Association*, San Jose, CA, 1997 Edition.

[2] K. R. Lakshmikumar, R. A. Hadaway and M. A. Copeland, "Characterisation and modelling of mismatch in MOS transistors for precision analogue design," *IEEE J. Solid State Circ.*, **SC-21** 1057 (1986).

[3] J.T. Horstmann, U. Hilleringmann and K. Goser, Matching Analysis of Deposition Defined 50-nm MOSFETs, *IEEE Trans. Electron Dev.* **45** 299 (1998).

[4] Wong H.-S. and Taur Y. "Three dimensional 'atomistic' simulation of discrete random dopant distribution effects in sub-0.1 mm MOSFETs," *Proc. IEDM'93. Dig. Tech. Papers.*, 705 (1993).

[5] J.-R. Zhou and D.K. Ferry, "Three-dimensional simulation of the effect of random dopant distribution on conductance for deep submicron devices," *Proc. 3rd Int. Workshop on Computational Electronics*, Plenum Press, New York, 74 (1994).